Connecting the pygmy dipole resonance to the neutron skin

V. Baran,[1,*] M. Colonna,[2] M. Di Toro,[2,3] A. Croitoru,[1] and D. Dumitru[1]

[1]*Faculty of Physics, University of Bucharest, Romania*
[2]*Laboratori Nazionali del Sud, INFN, I-95123 Catania, Italy*
[3]*Physics and Astronomy Department, University of Catania, Italy*

We study the correlation between the neutron skin development and the low-energy dipole response associated with the pygmy dipole resonance (PDR) in connection with the properties of symmetry energy. We perform our investigation within a microscopic transport model based on the Landau-Vlasov kinetic equation by employing three different equations of state in the isovector sector. Together with the giant dipole resonance, for all studied systems, we identify a PDR collective mode whose energy centroid is very well described by the parametrization $E_{\text{PDR}} = 41A^{-1/3}$. A linear correlation between the energy-weighted sum rule (EWSR) associated to PDR and the neutron skin thickness is evidenced. An increase of 15 MeV fm^2 of EWSR, in correspondence to a change of 0.1 fm of the neutron skin size, is obtained. We conjecture that different nuclei having close neutron skin sizes will exhaust the same EWSR in the pygmy region. This suggests that a precise experimental estimate of the total EWSR exhausted by the PDR allows the determination of the neutron skin size, constraining the slope parameter of the symmetry energy.

PACS number(s): 21.65.Ef, 24.10.Cn, 24.30.Gd, 25.20.Dc

I. INTRODUCTION

The nuclear symmetry energy, which originates from both Pauli correlations and the specific features of nuclear forces, accounts for the effects related to the difference between the number of protons Z and neutrons N of the system. It appears in the expression of total energy per particle, $\frac{E}{A}(\rho, I) = \frac{E}{A}(\rho) + \frac{E_{\text{sym}}}{A}(\rho)I^2$, factorizing the isospin parameter $I = \frac{N-Z}{A}$, where ρ is the nucleon density. Several features of atomic nuclei [1,2] and neutron stars [3] are determined by this quantity and one of the major tasks of recent experimental and theoretical investigations is to determine a consistent density parametrization of the symmetry energy which can provide a unified picture of nuclear properties below saturation as well as at large compression of asymmetric nuclear matter [4].

The fragmentation facilities at GANIL, GSI, MSU, and RIKEN, allowing for the study of very neutron-rich systems, stimulated new investigations along this direction. In this context, understanding the exotic modes of excitation [5] and the role of the neutron skin on the collective dynamics in nuclei far from stability is a challenge in modern nuclear physics [6–8]. Indeed, several experiments performed during the past 10 years reported the occurrence of an electric dipole ($E1$) response well below the giant dipole resonance (GDR), more clearly evidenced in neutron-rich nuclei [9–15]; see Refs. [16,17] for recent overviews. It manifests as a resonant-like shape exhausting few percentages of the dipolar energy-weighted sum rule (EWSR) and its controversial nature attracted a considerable interest for theory too [18]. The pygmy dipole resonance (PDR) was interpreted as a collective motion in phenomenological, hydrodynamic descriptions [19]; in nonrelativistic microscopic models [20–23]; or in transport models [24–26]. Also in a relativistic microscopic approach

[27] it was observed that the dipole spectra of even-even Ni and Sn isotopes show two well-separated collective structures, the lower one being identified with pygmy resonance, consistent with previous results based on relativistic quasi-particle random-phase approximation (RPA) [28–30]. Other studies, however, associate the concentration of strength to the contributions from single-particle-type excitations excluding coherent, collective properties [31,32]. It is possible that in the low-energy region the dipolar response manifests both single-particle and collective features. Moreover, a fragmentation of the $E1$ response is expected to determine a weakening of the collectivity [33,34].

A promising approach aiming to clarify the nature of PDR as well as the role of the symmetry energy and the neutron skin is based on a systematic analysis of the influence of the neutron excess on observables as the energy centroid or the low-energy $E1$ strength. Following this approach, several experimental investigations have been focused on the study of Ca [35], Ge [36], and Mo [37] isotopes as well as of $N = 50$ [38] and $N = 82$ isotones [39]. From the measurements for stable Sn isotopes [40–43] and neutron-rich systems $^{129-132}$Sn and ^{133,134}Sb [13], a trend of strength increasing with the neutron-proton asymmetry I^2 was reported. A threshold value of the isospin I, beyond which a sizable fraction of the pygmy strength appears, was related to the skin development [13]. The goal of this paper is to address the connection between the development of the neutron skin and the emergence of a low-energy $E1$ response in relation with the symmetry energy density dependence, a subject under intense debate during the past few years.

Theoretically, in a semiphenomenological description using a Hartree-Fock-Bogoliubov (HFB) treatment within the quasiparticle-phonon model (QPM) [44] for the neutron-rich Sn isotopes from ^{120}Sn to ^{132}Sn, it was stressed that the concentration of $E1$ strength, evidenced between 6 and 8 MeV, cannot be considered a low-energy tail of GDR.

*baran@ifin.nipne.ro

The corresponding states, having a genuine character with a dominance of neutron excitations, were considered noncollective. The evolution of the strength distribution and of the energy location was closely related to the features of neutron mantle enclosing the more isospin symmetric core. However, in a nonrelativistic RPA treatment [20] for zirconium isotopes, the investigation of the role played by the neutrons in excess has shown that these strongly contribute to the $E1$ excitation at about 8.5 MeV and make it collective. Moreover, the analysis [23] of neutron and proton contributions to PDR, based on a nonrelativistic self-consistent HF + RPA approximation, indicates that the pattern of the PDR changes with the increasing neutron number, becoming a quite collective resonant oscillation of the neutron skin. It was noticed a large collectivity of low-energy dipole states in ^{68}Ni and ^{132}Sn displaying a mixed isovector-isoscalar motion.

Piekarewicz [45] raised the important question if a strong correlation between the neutron skin and the low-energy $E1$ strength can be distinguished. For Sn isotopes, within a relativistic RPA model, he concluded that the fraction of EWSR acquired in the energy region between 5 MeV and 10 MeV manifests a linear dependence with the neutron skin size up to mass $A = 120$ followed by a mild anticorrelation. However, such strong correlation was questioned in Ref. [46]. The authors introduced an investigation based on a covariance analysis aimed to identify a set of good indicators that correlate very well with the isovector properties and suggested that the low-energy $E1$ strength is very weakly correlated with the neutron skin while the dipolar polarizability should be a much stronger indicator of isovector properties. This intriguing finding was challenged recently [47] in the relativistic RPA approach with mixed results. A strong correlation between the neutron skin thickness of ^{208}Pb and the dipole polarizability of ^{68}Ni was indeed reported. But a strong correlation was also claimed between the skin thickness of ^{208}Pb and low-energy $E1$ features, including the strength and dipole polarizability associated to the pygmy mode, identified in ^{68}Ni as exhausting about 5%–8% of the EWSR.

Here we shall address these controversial issues, proposing an investigation based on a semiclassical transport model. Because the neutron skin is an isovector indicator, we employ three different parametrizations with the density of the symmetry term and perform a comparative study in a model based on the Landau theory of Fermi liquids where the dynamics of the nucleons is described by Landau-Vlasov kinetic equations. In this paper we first explore the properties of the neutron skin and its sensitivity to the density dependence of symmetry energy. Then we determine the $E1$ strength function and study the mass dependence of the PDR peak. Finally, we estimate the EWSR exhausted by the PDR and discuss its relation with the neutron skin thickness. Since, as in the case of GDR, the evolution with mass of the low-energy $E1$ response provides an additional insight upon the nature of the mode, we shall consider the systems ^{48}Ca, ^{68}Ni, ^{86}Kr, and ^{208}Pb, as well as a chain of Sn isotopes, ^{108,116,124,132,140}Sn.

II. THEORETICAL FRAMEWORK

Having as main ingredients the fermionic nature of the constituents and the self-consistent mean-field, the Vlasov

equation represents the semiclassical limit of time-dependent Hartree-Fock (TDHF) and, for small-oscillations, of the RPA equations. While the model is unable to account for effects associated with the shell structure, our self-consistent approach is suitable to describe robust quantum modes, of zero-sound type, in both nuclear matter and finite nuclei. It provides important information about the dynamics of such collective modes, allowing for a systematic study over an extended mass and isospin domain. In this context we notice that in a TDHF study with a Skyrme interaction [48] a pygmylike peak was identified for the deformed ^{34}Mg at around 10 MeV. From time-dependent density plots it was recognized as a superimposed surface mode not fully coupled to the bulk motion. Similarly, studies based on Landau-Vlasov equations were also inquiring on the collective nature of PDR [24,49] and on the role of the symmetry energy on its dynamics [25]. It was observed that, as in the TDHF investigation, a pygmylike collective motion in ^{132}Sn manifests. Moreover, it was found that the symmetry energy does not affect the energy centroid but influences the EWSR acquired by it.

The two coupled Landau-Vlasov kinetic equations for neutrons and protons,

$$\frac{\partial f_q}{\partial t} + \frac{\mathbf{p}}{m} \frac{\partial f_q}{\partial \mathbf{r}} - \frac{\partial U_q}{\partial \mathbf{r}} \frac{\partial f_q}{\partial \mathbf{p}} = I_{\text{coll}}[f_n, f_p], \quad (1)$$

determine the time evolution of the one-body distribution functions $f_q(\vec{r}, \vec{p}, t)$, with $q = n, p$ [1]. In the following we shall switch-off the collision integral but we have tested that the results are not strongly influenced, as expected, when it is included. For the nuclear mean field we consider a Skyrme-like (SKM*) parametrization,

$$U_q = A \frac{\rho}{\rho_0} + B \left(\frac{\rho}{\rho_0} \right)^{\alpha+1} + C(\rho) \frac{\rho_n - \rho_p}{\rho_0} \tau_q$$
$$+ \frac{1}{2} \frac{\partial C}{\partial \rho} \frac{(\rho_n - \rho_p)^2}{\rho_0}, \quad (2)$$

with $\tau_n(\tau_p) = +1(-1)$. The saturation properties of the symmetric nuclear matter, $\rho_0 = 0.16$ fm^{-3}, $E/A = -16$ MeV and a compressibility modulus $K = 200$ MeV, are reproduced if the values $A = -356$ MeV, $B = 303$ MeV, $\alpha = 1/6$ are fixed. Concerning the density dependence of the symmetry energy, we consider, in the mean-field structure, different parametrizations of $C(\rho)$. While keeping the value of symmetry energy at saturation almost the same, we shall allow for three different dependencies with density away from equilibrium. For the asystiff equation of state (EOS) $C(\rho)$ is constant, $C(\rho) = 32$ MeV. Then the symmetry energy $E_{\text{sym}}/A = \frac{\epsilon_F}{3} + \frac{C(\rho)}{2} \frac{\rho}{\rho_0}$ at saturation takes the value $E_{\text{sym}}/A = 28.3$ MeV while the slope parameter $L = 3\rho_0 \frac{dE_{\text{sym}}/A}{d\rho}|_{\rho=\rho_0}$ is $L = 72$ MeV. The asysoft case corresponds to a Skyrme-like, SKM*, parametrization with $\frac{C(\rho)}{\rho_0} = (482 - 1638\,\rho)$ MeV fm^3, which leads to a small value of the slope parameter $L = 14.4$ MeV. Last, for the asy-superstiff EOS, $\frac{C(\rho)}{\rho_0} = \frac{32}{\rho_0} \frac{2\rho}{(\rho+\rho_0)}$, the symmetry term increases rapidly around saturation density, being characterized by a value of the slope parameter $L = 96.6$ MeV.

The integration of the transport equations is based on the test-particle (or pseudoparticle) method, with a number of
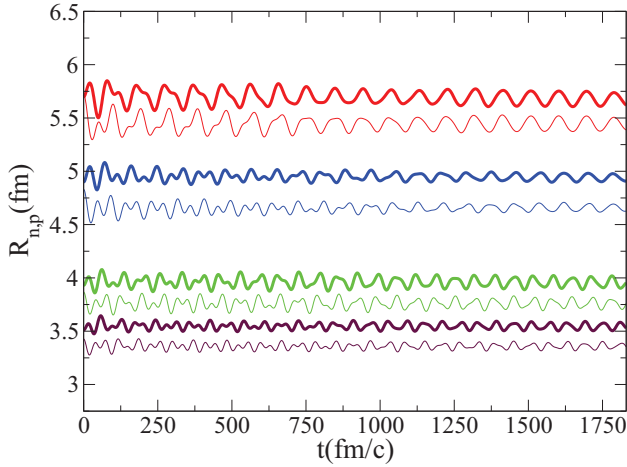
FIG. 1. (Color online) The time evolution of the neutron mean-square radius R_n (thick lines) and of the proton mean-square radius R_p (thin lines) after a weak perturbation of the ground state. From the top the pairs of lines correspond to ^{208}Pb (red), ^{132}Sn (blue), ^{68}Ni (green), and ^{48}Ca (maroon). The asystiff EOS case.

1300 test particles per nucleon in the case of Sn isotopes, ensuring in this way a good spanning of the phase space. This method is able to reproduce accurately the equation of state of nuclear matter and provide reliable results regarding the properties of nuclear surface [50] and ground-state energy for finite nuclei [51].

Since in the next section we shall explore the possible correlations between the properties of PDR and the neutron skin, we present here the predictions of the model for the neutron and proton distributions for different asy-EOS. From the one-body distribution functions one obtains the local densities: $\rho_q(\vec{r}, t) = \int \frac{2 d^3 \mathbf{p}}{(2\pi\hbar)^3} f_q(\vec{r}, \vec{p}, t)$ as well as the quadratic radii $\langle r_q^2 \rangle = \frac{1}{N_q} \int r^2 \rho_q(\vec{r}, t) d^3 \mathbf{r}$ and the width of the neutrons skin $\Delta R_{np} = \sqrt{\langle r_n^2 \rangle} - \sqrt{\langle r_p^2 \rangle} = R_n - R_p$.

An efficient method to extract the values of R_n and R_p is by observing their time evolution after a gentle monopolar perturbation. Both quantities perform small oscillations around equilibrium values and we remark that the numerical simulations keep a very good stability of the dynamics for at least 1800 fm/c; see Fig. 1. Using this procedure, we obtain for the charge mean-square radius of ^{208}Pb a value around $R_p = 5.45$ fm, to be compared with the experimental value $R_{p,\text{exp}} = 5.50$ fm. For Sn isotopes we display the mass dependence of R_n, R_p in Fig. 2(a) and of ΔR_{np}, respectively, in Fig. 2(b). The charge radii predictions from the three asy-EOS virtually coincide and we notice a good agreement with the experimental data reported in Refs. [52,53]. However, the calculations somehow underestimate the charge radii at smaller A and tend to overestimate it towards larger A, thus providing a stronger rise tendency than observed experimentally. For all adopted parametrizations the values of the neutron skin thickness are within the experimental errors bars; see the data presented in Ref. [54] for the stable Sn nuclei. In the case of ^{208}Pb we find $\Delta R_{np} = 0.19$ fm for asysoft, $\Delta R_{np} = 0.25$ fm for asystiff, and $\Delta R_{np} = 0.27$ fm for asysuperstiff EOS while for ^{68}Ni
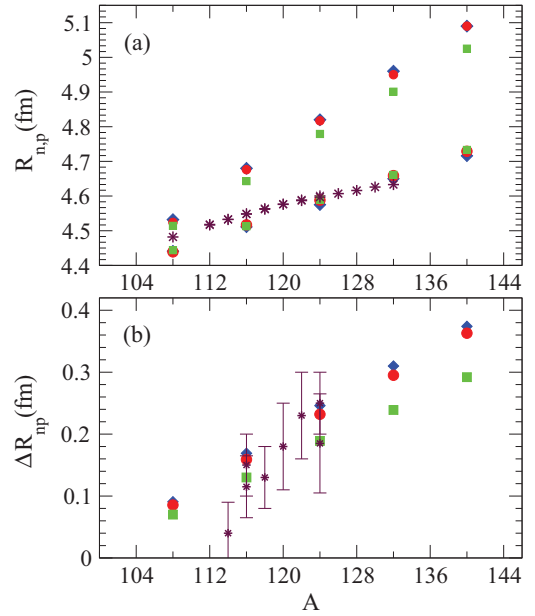

FIG. 2. (Color online) (a) The neutron and proton mean-square radius for Sn isotopes: asysoft (the green squares), asystiff (the red circles), and asysuperstiff (the blue diamonds) EOS. The stars are experimental data from Refs. [52,53]. (b) The neutron skin thickness as a function of mass for Sn isotopes: asysoft (green squares), asystiff (the red circles), and asysuperstiff (the blue diamonds). The stars and the error bars (maroons) are experimental data from Ref. [54].

the corresponding values are $\Delta R_{np} = 0.17, 0.19, 0.20$ fm. As expected, the neutron skin thickness increases with the slope parameter L, an effect related to the tendency of the system to stay more isospin symmetric even at lower densities when the symmetry energy changes slowly below saturation, as in the case of the asysoft EOS.

III. COLLECTIVE PYGMY DIPOLAR RESPONSE

We study the $E1$ response considering a GDR-like initial condition [25], determined by the instantaneous excitation $V_{\text{ext}} = \eta \delta(t - t_0) \hat{D}$ at $t = t_0$ [55]. This situation corresponds to a boost of all neutrons against all protons while keeping the center of mass (c.m.) at rest. Here $\hat{D}$ is the dipole operator. If $|\Phi_0\rangle$ is the state before perturbation, then the excited state becomes $|\Phi(t_0)\rangle = e^{i\eta\hat{D}}|\Phi_0\rangle$. The value of η can be related to the initial expectation value of the collective dipole momentum $\hat{\Pi}$,

$$\langle \Phi(t_0)|\hat{\Pi}|\Phi(t_0)\rangle = \hbar\eta \frac{NZ}{A}. \tag{3}$$

Here $\hat{\Pi}$ is canonically conjugated to the collective coordinate $\hat{X}$, which defines the distance between the center of mass of protons and the center of mass of neutrons, i.e., $[\hat{X}, \hat{\Pi}] = i\hbar$ [49]. Then the strength function

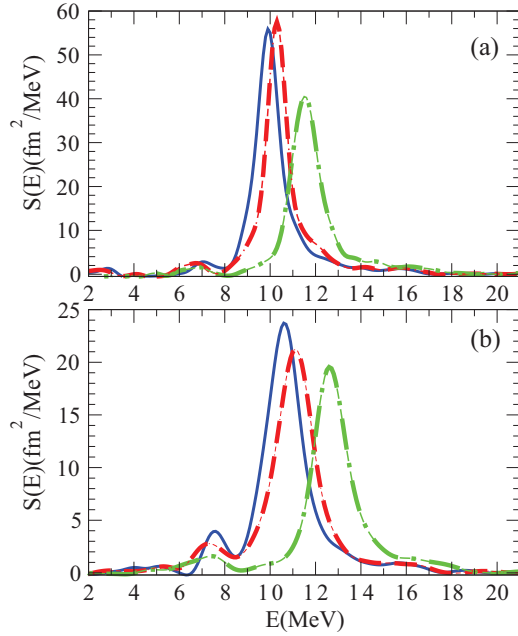$$S(E) = \sum_{n>0} |\langle n|\hat{D}|0\rangle|^2 \delta(E - (E_n - E_0)), \tag{4}$$

FIG. 3. (Color online) The strength function for ^{208}Pb (a) and ^{140}Sn (b) for asysoft [the green (dot-dashed) lines], aystiff [the red (dashed) lines], and asysuperstiff [the blue (solid) lines] EOS.
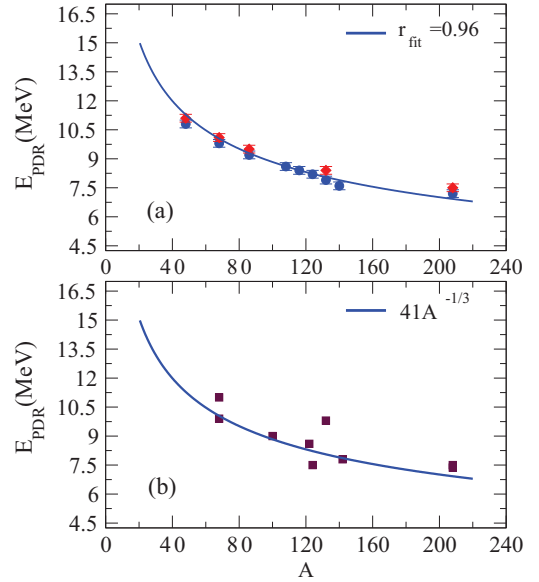

FIG. 4. (Color online) (a) The energy centroid of PDR as a function of mass. The blue circles and red diamonds are the predictions of the model; see the text. The best fit, the solid (blue) line, corresponds to the parametrization $E_{PDR} = 41A^{-1/3}$. r_{fit} refers to the correlation coefficient. (b) The energy centroid of PDR from experimental data. The maroon squares are experimental data points; see the text. The solid blue line corresponds to the parametrization $41A^{-1/3}$.

where E_n are the excitation energies of the states $|n\rangle$ while E_0 is the energy of the ground state $|0\rangle = |\Phi_0\rangle$, is obtained in our approach from the imaginary part of the Fourier transform of the time-dependent expectation value of the dipole momentum $D(t) = \frac{NZ}{A}X(t) = \langle\Phi(t)|\hat{D}|\Phi(t)\rangle$ as

$$S(E) = \frac{\text{Im}(D(\omega))}{\pi\eta\hbar}, \quad (5)$$

where $D(\omega) = \int_{t_0}^{t_{max}} D(t)e^{i\omega t}dt$. We consider the initial perturbation along the z axis and follow the dynamics of the system until $t_{max} = 1830$ fm/c. At $t = t_0 = 30$ fm/c we extract the collective momentum and determine η. A filtering procedure, as described in Ref. [56], was applied in order to eliminate the artifacts resulting from a finite-time domain analysis of the signal. A smooth cut-off function was introduced such that $D(t) \rightarrow D(t)\cos^2(\frac{\pi t}{2t_{max}})$. For the three asy-EOS the $E1$ strength functions of ^{208}Pb and ^{140}Sn are represented in Fig. 3. As a test of the quality of our method we compared the numerically estimated value of the first moment $m_1 = \int_0^\infty ES(E)dE$ with the value predicted by the Thomas-Reiche-Kuhn (TRK) sum rule $m_1 = \frac{\hbar^2}{2m}\frac{NZ}{A}$. In all cases the difference was only a few percentages.

The energy peak of the PDR for ^{208}Pb, see Fig. 3(a), is located around 7–7.5 MeV, in good agreement with experimental data which indicate $E_{PDR,Pb} = 7.36$ MeV [14]. For ^{68}Ni we obtain 9.8 MeV, quite close to the recent reported data $E_{PDR,Ni} = 9.9$ MeV [57]. We observe that the GDR energy centroid is underestimated in comparison with experimental data, a fact related with the choice of the interaction which has not an effective mass [58]. In any case, a clear dependence on the slope parameter manifests as a consequence of the isovector nature of the mode. This feature shows that also

the symmetry energy values below saturation are affecting the dipole oscillations of the finite systems. Figure 4(a) displays the predicted position of the PDR energy centroid as a function of mass for all studied systems (blue circles). Since in all cases a very weak influence of the symmetry energy on the PDR peak was observed, we take the average of the values corresponding to the three asy-EOS. Then the error bars represent the deviation of the determined values from the average. In addition, by using the same procedure, we represent the position of the PDR energy peaks as results from the power spectrum analysis of the pygmy dipole $D_y(t)$ after a pygmylike initial condition, see Ref. [25] (red diamonds). The differences between the two methods are within a half of a MeV. An appropriate parametrization, obtained from the fit of numerical results, is

$$E_{PDR} = 41A^{-1/3} \text{ MeV}, \quad (6)$$

quite close to what is expected in the harmonic oscillator shell-model (HOSM) approach [49]. In Fig. 4(b) this parametrization is compared with the experimental data available from the works where information about the position of the low-energy $E1$ centroid was reported (maroon square).[1] The formula seems to describe quite well the position of the low-energy centroid observed experimentally for several systems. While the isovector residual interaction pushes up the value of the

---

[1]For ^{68}Ni from Refs. [12,57]; for ^{100}Mo from Ref. [37]; for ^{122}Sn from Ref. [43]; for ^{124}Sn from Ref. [42]; for ^{132}Sn from Ref. [11]; for ^{142}Nd from Ref. [59]; for ^{208}Pb from Refs. [14,15].

GDR energy, it seems that the PDR energy centroid is not much affected by this part of the interaction. This feature may explain the better agreement with experimental observations in comparison with the GDR case. The agreement also suggests that the PDR peak energy should not be significantly influenced by the momentum dependence of the interaction. Let us mention that for Ni, Sn, and Pb isotopic chains, based on a HFB and RQRPA treatment, Paar *et al.* [60] studied the isotopic dependence of the PDR energy and a collective mode with the energy centroid around 10 MeV for ^{68}Ni, 8 MeV for ^{132}Sn, and 7.5 MeV for ^{208}Pb was predicted. A comparison with our results shows a good concordance between the two theoretical approaches for the position of the PDR energy centroid.

Having obtained the strength function, we can calculate the nuclear dipole polarizability,

$$\alpha_D = 2e^2 \int_0^\infty \frac{S(E)}{E} dE, \qquad (7)$$

as an additional test of the numerical method. In the case of ^{68}Ni α_D varies from 4.1 fm^3 to 5.7 fm^3 when we pass from asysoft to asysuperstiff EOS while for ^{208}Pb it changes from 21.1 fm^3 to 28.6 fm^3. Since for proposed interactions the position of the GDR peak is below the experimental observations, we expect that the values of the polarizabilities to be somehow overestimated in comparison with data. Experimentally, the dipole polarizability is below 4 fm^3 for ^{68}Ni [57] and around 20 fm^3 for ^{208}Pb [14]. We display this quantity as a function of mass and asy-EOS in Fig. 5. For a given system, the larger the neutron skin thickness, the greater the value of the dipole polarizability obtained.

The EWSR exhausted by the PDR is calculated by integrating over the low-energy resonance region as follows:

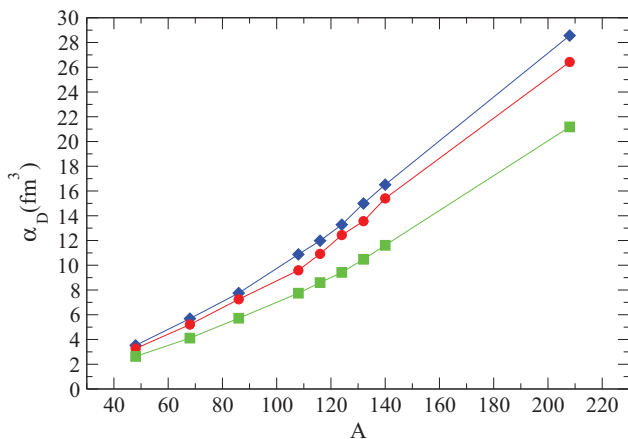$$m_{1,y} = \int_{\text{PDR}} E S(E) dE. \qquad (8)$$

FIG. 5. (Color online) The dipole polarizability as a function of mass for asysoft (the green squares), asystiff (the red circles), and asysuperstiff (the blue diamonds) EOS. All systems mentioned in text are included.
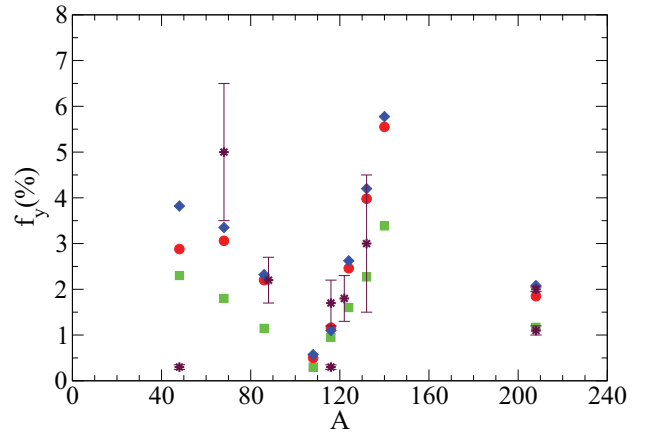

FIG. 6. (Color online) The fraction of EWSR exhausted by PDR as a function of mass for asysoft (green squares), asystiff (red circles), and asysuperstiff (blue diamonds) EOS for the systems ^{48}Ca, ^{68}Ni, ^{86}Kr, ^{108}Sn, ^{116}Sn, ^{124}Sn, ^{132}Sn, ^{140}Sn, and ^{208}Pb. The stars (maroon) are experimental data points obtained by various methods for ^{48}Ca, ^{68}Ni, ^{88}Sr, ^{116}Sn, ^{122}Sn, ^{132}Sn, and ^{208}Pb, reported in Ref. [17].

We carefully determined the limits of the pygmy resonance region, identifying the minima of the response around the PDR centroid. When an overlap with the GDR region exists, the contribution from the GDR tail is substracted. In Fig. 6 the fraction $f_y = \frac{m_{1y}}{m_1}$ exhausted by the pygmy dipole resonance as a function of mass is reported. Some comments are valuable when we compare our results with experimental data concerning the same quantity obtained from various experiments, as presented in Fig. 26 of Ref. [17]. For ^{48}Ca the fraction is obtained experimentally from the strength observed to 10 MeV and is below 0.3%. However, our calculations point out that the PDR is mainly above 10 MeV and we obtain a fraction, depending on the asy-EOS, between 2.3% and 3.8%. For ^{68}Ni, our model, with a calculated fraction between 1.8% and 3.5%, underestimates the experimental value, which is around $f_y = 5\%$. In the mass region $A = 88$–90 the experimental fraction is situated at $f_y = 2\%$ and for ^{86}Kr we obtain between 1.1% and 2.3%. For the stable Sn isotopes, in the mass region $A = 116$–124, the fraction measured experimentally is between 1.2% and 2.2% while our calculations suggest values between 0.95% and 1.1% for ^{116}Sn and between 1.6% and 2.6% for ^{124}Sn. In the case of ^{132}Sn our results are between 2.2% and 4.2% while experimentally the reported fraction is around 3%. Finally, for ^{208}Pb we obtain a fraction between 1% and 2%, which is the same range as that in the existing experimental data. We conclude that, despite the fact that our approach has the tendency to underestimate the experimental results (except for Calcium, for the reasons discussed above), the model reveals that a substantial part of the total fraction f_y exhausted in the low-energy region can be attributed to the collective PDR.

We investigate now if some correlation between the absolute value of EWSR exhausted in the PDR region and the development of neutron skin manifests in our approach. The dependence of the moment $m_{1,y}$ on the neutron skin thickness is shown in Fig. 7, where the information concerning all
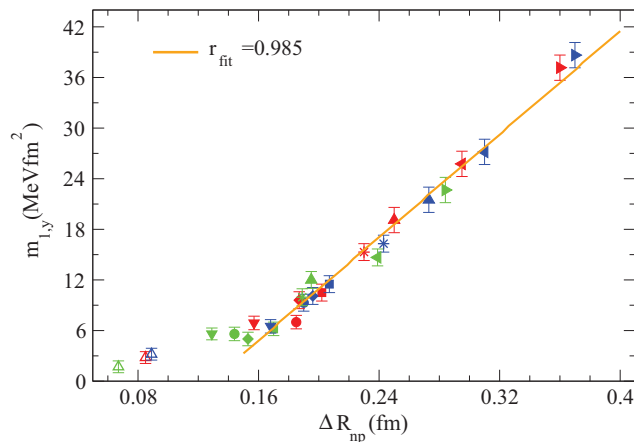
FIG. 7. (Color online) The EWSR exhausted by PDR as a function of neutron skin for ^{108}Sn (empty up-triangles), ^{116}Sn (down-triangles), ^{124}Sn (stars), ^{132}Sn (left triangles), ^{140}Sn (right triangles), ^{48}Ca (circles), ^{68}Ni (squares), ^{86}Kr (diamonds), ^{208}Pb (full up-triangles) for asysoft (green), asystiff (red), and asysuperstiff (blue) EOS. The error bars are related to the uncertainties in defining the integration domain for the PDR response. $r_{\rm fit}$ refers to the correlation coefficient.

mentioned systems was included. The error bars are associated with the uncertainty in the identification of the limits of the pygmy resonance region. While below 0.15 fm the EWSR acquired by the PDR manifests a saturation tendency, above this value a linear correlation arises. For the same nucleus, when we pass from the asysuperstiff to asysoft parametrization, the neutron-skin shrinks and, correspondingly, the value of $m_{1,y}$ decreases. This behavior is in agreement with the results reported in Ref. [61] in a self-consistent RPA approximation based on relativistic energy-density functionals. Moreover, we notice that the variation rate appears to be system independent, obtaining an increase of 15 MeV fm^2 of the exhausted EWSR, versus a change of 0.1 fm of the neutron skin width. Such features suggest that the acquired EWSR should not differ too much even for different nuclei if they have close values of neutrons skin thickness. These findings look qualitatively in agreement with those of Inakura *et al.* [62], based on systematic calculations within a RPA treatment with a SkM* Skyrme functional, where a linear correlation of the fraction of EWSR exhausted in the the energy region up to 10 MeV and neutron skin thickness was evidenced for several isotopic chains.

However, some differences are also worth mentioning. While we observe the total amount of EWSR exhausted in the PDR region, m_{1y}, manifests a system-independent, linear dependence with the neutron skin thickness, with a slope $s = 150$ MeV fm, Inakura *et al.* deduce a linear correlation of the fraction f_y as a function of ΔR_{np}. In this case, the corresponding universal rate is 0.18–0.20 fm^{-1} for even-even nuclei with $8 \leqslant Z \leqslant 40$. To establish a connection between the two approaches, we shall assume that within a specific isotopic chain the ratio NZ/A does not change too much, i.e., the value of m_1 is approximately the same for all those nuclei. With this approximation, for a fixed isotopic chain, the

two predictions are similar, i.e., an universal slope for f_y is equivalent with an universal slope for m_{1y}. Consequently, in the Inakura approach, it can be deduced that the value of the slope s is around 70 MeV fm for Ca isotopes, 95 MeV fm for Ni chain, and 120 MeV fm for Kr isotopes.

We also remark that, in Ref. [62], for very neutron-rich systems a mild anticorrelation of f_y with the neutron skins begin to manifest, similarly to the results of Refs. [45,63]. This feature is missing in our model. We obtain a continuous rise of $m_{1,y}$ with the neutron skin size, in concordance with other studies based on microscopic treatments [44,64]. One can relate these differences to some shell and angular-momentum effects but further investigations are required for a definite answer.

IV. CONCLUSIONS

Summarizing, we addressed some of the open questions raised recently [17] regarding the nature of the PDR. By performing a systematic investigation over an extended mass domain, new features, providing a more complete picture of the PDR dynamics, were evidenced. In a microscopic transport approach, a low-energy dipole collective mode occurs as a ubiquitous property of all investigated systems. The analysis leads us to a dependence of the PRD energy centroid with mass very well described by the parametrization $E_{\rm PDR} = 41A^{-1/3}$, in agreement with several recent experimental results. This indicates a close connection with the distance between major shells, $\hbar\omega_0 = 41A^{-1/3}$, and a weak influence of the residual interaction in the isovector sector. Such behavior can be related to the isoscalar-like nature of this mode. We notice that the EWSR exhausted by the collective pygmy dipole depends on the symmetry energy slope parameter L and represents a significant part of the value determined experimentally. From our investigation, a universal, linear correlation of m_{1y} with the neutron skin thickness emerges. It appears as a very specific signature, showing that the neutrons which belong to the skin play an essential role in shaping the $E1$ response in the PDR region. However, this fact should not lead to an oversimplified picture of the PDR, as corresponding only to the oscillations of the excess neutrons against an inert isospin symmetric core. Within our transport model, the dynamical simulations show a more complex structure of the PDR [25], which includes an isovector excitation of the core and the neutrons skin oscillation. We consider that the new findings presented here can be useful for further, systematic experiments searching for this, quite elusive, mode. A precise estimate of the EWSR acquired by the PDR can provide indications about the neutron skin size, which in turn will add more constraints on the slope parameter L of the symmetry energy.

[1] V. Baran, M. Colonna, M. Di Toro, and V. Greco, Phys. Rep. **410**, 335 (2005).

[2] Li Bao-An, Lie-Wen Chen, and Che Ming Ko, Phys. Rep. **464**, 113 (2008).

[3] A. W. Steiner, M. Prakash, J. M. Lattimer, and P. J. Ellis, Phys. Rep. **411**, 325 (2005).

[4] M. Di Toro, V. Baran, M. Colonna, and V. Greco, J. Phys. G: Nucl. Part. Phys. **37**, 083101 (2010).

[5] N. Paar, D. Vretenar, E. Khan, and G. Colo, Rep. Prog. Phys. **70**, 691 (2007).

[6] P. Van Isacker, M. A. Nagarajan, and D. D. Warner, Phys. Rev. C **45**, R13 (1992).

[7] A. Carbone, G. Colo, A. Bracco, L. G. Cao, P. F. Bortignon, F. Camera, and O. Wieland, Phys. Rev. C **81**, 041301(R) (2010).

[8] O. Wieland and A. Bracco, Prog. Part. Nucl. Phys. **66**, 374 (2011).

[9] T. Hartmann, J. Enders, P. Mohr, K. Vogt, S. Volz, and A. Zilges, Phys. Rev. Lett. **85**, 274 (2000).

[10] T. Hartmann, J. Enders, P. Mohr, K. Vogt, S. Volz, and A. Zilges, Phys. Rev. C **65**, 034301 (2002).

[11] P. Adrich et al., Phys. Rev. Lett. **95**, 132501 (2005).

[12] O. Wieland et al., Phys. Rev. Lett. **102**, 092502 (2009).

[13] A. Klimkiewicz et al., Phys. Rev. C **76**, 051603(R) (2007).

[14] A. Tamii et al., Phys. Rev. Lett. **107**, 062502 (2011).

[15] T. Kondo et al., Phys. Rev. C **86**, 014316 (2012).

[16] T. Aumann and T. Nakamura, Phys. Scr. T **152**, 014012 (2013).

[17] D. Savran, T. Aumann, and A. Zilges, Prog. Part. Nucl. Phys. **70**, 210 (2013).

[18] N. Paar, J. Phys. G: Nucl. Part. Phys. **37**, 064014 (2010).

[19] R. Mohan, M. Danos, and L. C. Biedenharn, Phys. Rev. C **3**, 1740 (1971); Y. Suzuki, K. Ikeda, and H. Sato, Prog. Theor. Phys. **83**, 180 (1990); S. I. Bastrukov et al., Phys. Lett. B **664**, 258 (2008).

[20] G. Co', V. De Donno, C. Maieron, M. Anguiano, and A. M. Lallena, Phys. Rev. C **80**, 014308 (2009).

[21] E. G. Lanza, A. Vitturi, M. V. Andres, F. Catara, and D. Gambacurta, Phys. Rev. C **84**, 064602 (2011).

[22] X. Roca-Maza, G. Pozzi, M. Brenna, K. Mizuyama, and G. Colo, Phys. Rev. C **85**, 024601 (2012).

[23] E. Yuksel, E. Khan, and K. Bozkurt, Nucl. Phys. A **877**, 35 (2012).

[24] M. Urban, Phys. Rev. C **85**, 034322 (2012).

[25] V. Baran, B. Frecus, M. Colonna, M. Di Toro, Phys. Rev. C **85**, 051601 (2012).

[26] C. Tao, Y. G. Ma, G. Q. Zhang, X. G. Cao, D. Q. Fang, and H. W. Wang, Phys. Rev. C **87**, 014621 (2013).

[27] E. Litvinova, P. Ring, V. Tselyaev, and K. Langanke, Phys. Rev. C **79**, 054312 (2009).

[28] D. Vretenar, N. Paar, P. Ring, and G. A. Lalazissis, Nucl. Phys. A **692**, 496 (2001); D. Vretenar, T. Niksic, N. Paar, and P. Ring, ibid. **731**, 281 (2004).

[29] N. Paar, Y. F. Niu, D. Vretenar, and J. Meng, Phys. Rev. Lett. **103**, 032502 (2009).

[30] I. Daoutidis and P. Ring, Phys. Rev. C **83**, 044303 (2011).

[31] N. Tsoneva and H. Lenske, Phys. Rev. C **77**, 024321 (2008).

[32] P.-G. Reinhard and W. Nazarewicz, Phys. Rev. C **87**, 014324 (2013).

[33] D. Sarchi, P. F. Bortignon, and G. Colo, Phys. Lett. B **601**, 27 (2004).

[34] D. Gambacurta, M. Grasso, and F. Catara, Phys. Rev. C **84**, 034301 (2011).

[35] T. Hartmann, M. Babilon, S. Kamerdzhiev, E. Litvinova, D. Savran, S. Volz, and A. Zilges, Phys. Rev. Lett. **93**, 192501 (2004).

[36] A. Jung et al., Nucl. Phys. A **584**, 103 (1995).

[37] G. Rusev et al., Eur. Phys. J. A **27**, 171 (2006).

[38] R. Schwengner et al., Phys. Rev. C **76**, 034321 (2007); **78**, 064314 (2008); **87**, 024306 (2013).

[39] S. Volz et al., Nucl. Phys. A **779**, 1 (2006).

[40] K. Govaert et al., Phys. Rev. C **57**, 2229 (1998).

[41] B. Ozel et al., Nucl. Phys. A **788**, 385c (2007).

[42] J. Endres et al., Phys. Rev. Lett. **105**, 212503 (2010).

[43] H. K. Toft et al., Phys. Rev. C **83**, 044320 (2011).

[44] N. Tsoneva et al., Phys. Lett. B **586**, 213 (2004).

[45] J. Piekarewicz, Phys. Rev. C **73**, 044325 (2006).

[46] P.-G. Reinhard and W. Nazarewicz, Phys. Rev. C **81**, 051303(R) (2010).

[47] J. Piekarewicz, Phys. Rev. C **83**, 034319 (2011).

[48] M. P. Brine, P. D. Stevenson, J. A. Mahrun, and P.-G. Reinhard, Int. J. Mod. Phys. E **15**, 1417 (2006).

[49] V. I. Abrosimov and O. I. Davydovs'ka, Ukr. J. Phys. **54**, 1068 (2009); V. Baran et al., Rom. J. Phys. **57**, 36 (2012).

[50] D. Idier, B. Benhassine, M. Farine, B. Remaud, and F. Sebille, Nucl. Phys. A **564**, 204 (1993).

[51] P. Schuck et al., Prog. Part. Nucl. Phys. **22**, 181 (1989).

[52] C. W. De Jager et al., At. Data Nucl. Data Tables **36**, 495 (1987); G. Audi and A. H. Wapstra, Nucl. Phys. A **595**, 409 (1995).

[53] I. Angeli and K. P. Marinova, At. Data Nucl. Data Tables **99**, 69 (2013).

[54] A. Krasznahorkay et al., Phys. Rev. Lett. **82**, 3216 (1999).

[55] F. Calvayrac, P. G. Reinhard, and E. Suraud, Ann. Phys. (NY) **225**, 125 (1997).

[56] P.-G. Reinhard, P. D. Stevenson, D. Almehed, J. A. Maruhn, and M. R. Strayer, Phys. Rev. E **73**, 036709 (2006).

[57] D. Rossi, INPC2013, Firenze, Italy, and private communication.

[58] E. Suraud, M. Pi, and P. Schuck, Nucl. Phys. A **482**, 187c (1988).

[59] C. T. Angell et al., Phys. Rev. C **86**, 051302(R) (2012).

[60] N. Paar et al., Phys. Lett. B **606**, 288 (2005).

[61] D. Vretenar, Y. F. Niu, N. Paar, and J. Meng, Phys. Rev. C **85**, 044317 (2012).

[62] T. Inakura, T. Nakatsukasa, and K. Yabana, Phys. Rev. C **84**, 021302(R) (2011).

[63] J. Liang, L. G. Cao, and Z. Y. Ma, Phys. Rev. C **75**, 054320 (2007).

[64] D. Pena Arteaga, E. Khan, and P. Ring, Phys. Rev. C **79**, 034311 (2009).